Front. Struct. Civ. Eng. 2019, 13(3): 557–568
https://doi.org/10.1007/s11709-018-0497-z

RESEARCH ARTICLE

Practical optimization of deployable and scissor-like structures using a fast GA method

M. SALAR[a], M. R. GHASEMI[a*], B. DIZANGIAN[b]

[a] *Department of Civil Engineering, University of Sistan and Baluchestan, Zahedan, Iran*

[b] *Department of Civil Engineering, Velayat University, Iranshahr, Iran*

[*] *Corresponding author. E-mail: mrghasemi@eng.usb.ac.ir*

ABSTRACT This paper addresses practical sizing optimization of deployable and scissor-like structures from a new point of view. These structures have been recently highly regarded for beauty, lightweight, determine behavior, proper performance against lateral loads and the ability of been compactly packaged. At this time, there is a few studies done considering practical optimization of these structures. Loading considered here includes wind and gravity loads. In foldable scissor-like structures, connections have a complex behavior. For this reason, in this study, the authors used the ABAQUS commercial package as an analyzer in the optimization procedure. This made the obtained optimal solutions highly reliable from the point of view of applicability and construction requirements. Also, to do optimization task, a fast genetic algorithm method, which has been recently introduced by authors, was utilized. Optimization results show that despite less weight for aluminum models than steel models, aluminum deployable structures are not affordable because they need more material than steel structures and cause more environmental damage.

KEYWORDS optimization, scissor-like structures, deployable structures, genetic algorithm, ABAQUS

1 Introduction

A deployable structure is one converted from a closed compact form into a known, expanded form wherein it is stable and can carry loads [1]. It is presently used in civil and aerospace engineering with such applications as morphing structures, foldable reflectors (antennas), temporary shelters, bridges. Since the deployment phase is to be considered, designs related to deployable structures are extensions of mainstream design practice in civil engineering. Besides, such additional tasks and constraints as element entanglement and path planning are needed in the design of deployable structures [2]. Common deployable systems in recent researches are pantographs which contain elements made of two rods connected (like scissor blades) at an intermediate node [3] that creates a pivotal connection to allow rods to rotate freely in the same plane while preventing all other degrees of freedom. Large pantographic structures can be created by joining a number of scissor-like structural elements.

Article history: Received Jan 6, 2018; Accepted Feb 12, 2018

In numerous structure-related studies, mention has been made of the name of the great Renaissance thinker and artist Leonardo da Vinci (1452–1519) who designed, for the first time, a simple, flat, expandable mechanism. But three-dimensional (3D) structures of this type were first developed by Emilio Perez Pinero who designed, in early 1960s, the foldable scissor-like spatial grid and patented it as an invention. He suggested single-/double-layer domes and flat grids for mobile theaters and public expo buildings. During his lifetime, he also designed and implemented a number of foldable structures including a foldable dome of 99 m span [4] for a mobile theater that needed tension cables for its stabilization and lacked stress in both open and closed configurations as well as during opening [1,5].

To stabilize structures (like Pinero's) that undergo opening-closing mechanism, use has to be made of locking tools which add extra members between nodes and apply external forces. External stabilization of large deployable structures is quite difficult and costly and requires trained, experienced manpower [6].

Pinero also collaborated with Salvador Daly in a project

to build a foldable sculpture with 84 glass pieces and super cube geometry. Escrig believes that this was the first example of a foldable space grid wherein the cover was connected to the entire structure. Pinero's work did not finish because of his untimely death, but his theory was pursued by others in the following years and was further developed by Valcarcel and Escrig [7], Calatrava [8], Ziegler [9], Hernández Zalewski [10], and Escrig [11].

After Pinero, Ziegler patented his invention [9] which was a foldable geodesic dome (Fig. 1), criticized Pinero's work, and proposed a method to stabilize the structural geometry without the need for lateral lockers. To reach this goal, he stated three important conditions on which basis he obtained new geometrical shapes, and succeeded in developing such components as sliding and spring-shaped load-bearing connections and removing intermediate connections in some scissor-like modules and the like. To create folding-opening conditions, Ziegler allowed some of his own-defined flexible elements to bend, but bent elements lose their load bearing capacity considerably because they are prone to buckling and rupture during loading. Additionally, most materials are deformed if they remain bent for a long time; however, Ziegler's method facilitated future studies [12].

The first researcher that introduced various types of pantograph foldable structures comprehensively and in details was Escrig [11] who stated how linear, grid, and spatial structures could be created using duplets (as the basic module of pantograph structures). Figure 2 shows some examples of geometric shapes designed by Escrig [11]. He then introduced different types of connections and how to open and close foldable structures, and eventually did a detailed study of the linear analysis of these structures. Although his work seems general and superficial, it has facilitated many researches in recent years [11].

Shan [13] was the first to present the most important research on the analysis of structures compatible with scissor-like elements. He introduced foldable structures in details, discussed their configurations, and presented their geometric design. A large part of his studies was on linear and nonlinear analysis of foldable pantograph structures. Considering a uniplet as a 3-node beam and applying support conditions, he extracted its stiffness matrix through which he presented a program for the analysis of foldable structures. Langbecker and Albermani [14] addressed the kinematic analysis of foldable barrels consisting of scissor-like units to extract constraints for their geometric design; effects of member size, depth to span ratio, and geometric defects were other issues they investigated.

Gantes et al. [6,15] used scissor-like elements to study deployable structures. Optimization (the best solution in a closed space where all objectives and constraints can be expressed mathematically) plus search methods help

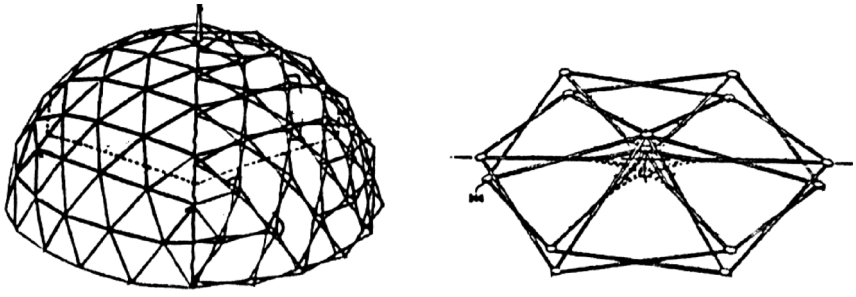

Fig. 1 Zeigler's collapsible dome and a basic unit [1]

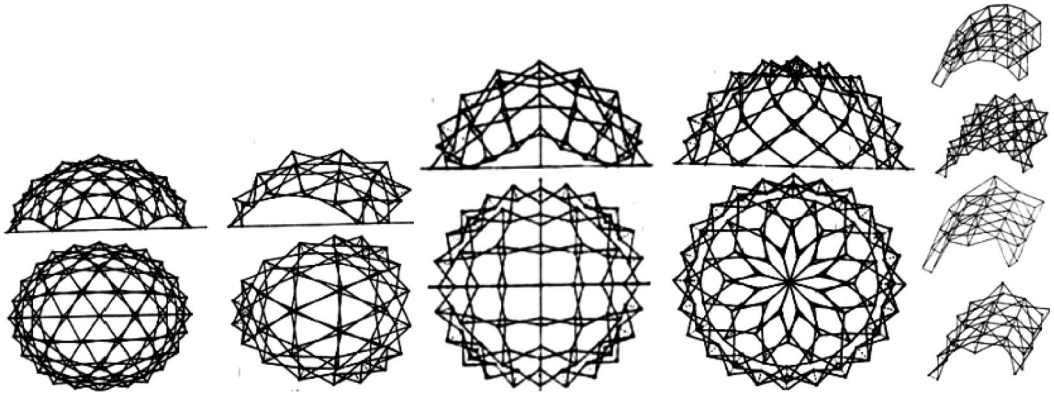

Fig. 2 Geometric shapes designed by Escrig [11]

engineers find candidate solutions for complex problems with a large space [16]. Scissor-hinge structures are among very common types of deployable structures.

2 Analysis of deployable structures

Numerical analyses are necessary for deployable structures because they differ from conventional structures in two main issues: (i) Their geometry is 3D while earlier analytical works have been confined to 2D frames having simple, rectangular geometric shapes; and (ii) they have hinged, pivotal connections that allow large, arbitrary member rotations while structures with rigidly connected bars are studied mainly through analytical methods.

When deployable structures are subjected to service loads, they may experience three potential failure modes: Strength, stiffness, and buckling. Factors deciding which one is the critical mode include structural system, span length, geometric details, and material properties. Predicting the governing failure mode in advance is not easy; therefore, all three possible modes should be considered during the design process. Strength failure in an "allowable stress" approach occurs when stresses are higher than a predefined maximum allowable value, but in an "ultimate strength" design approach, it is an overall bearing capacity failure. When deflections are larger than a given limit, the structure will experience stiffness failure.

Simple linear analysis methods can be used to study the first two failure modes, but since large axial forces in structure members cause buckling, and a small load increase can result in a rapid change in the shape of the structure, use has to be made of nonlinear analyses methods for the boundary conditions and service loading to detect buckling and calculate buckling loads. When pre-failure displacements are large, buckling can be associated with a limit point, but when the pre-buckling behavior is linear, it can be associated with a bifurcation point. In the latter case, a linearized buckling analysis can evaluate the buckling load with satisfactory accuracy [1].

3 Genetic algorithms

3.1 Background

Optimization of structures has always been a fast-developing area of research in the field of engineering optimization and has made notable progress in the last decade. One could categorize the structural optimization task into three general categories: (i) Sizing optimization, where the design variables consist of cross sectional area of elements [17,18]; (ii) configuration optimization, in which the nodal coordinates could be considered as design variables [19]; and (iii) topology optimization, that it optimizes material layout within a given design space where material is either present, indicated by 1, or absent, indicated by 0 [20–23].

Genetic algorithms (GAs), which were originally proposed by John Holland at the University of Michigan [24], are search procedures based on natural selection and survival of the fittest, and unlike many mathematical programming algorithms they do not require the evaluation of gradients of the objective function and constraints. The GA-based methods accept discrete and/or continuous design variables for the optimization process and are therefore very versatile. GAs are computationally simple, but powerful in their search for improvement, and they are not limited by restrictive assumptions about the search space, such as continuity or existence of derivatives. GAs are search procedures based on the mechanics of natural genetics and natural selection. They combine the concept of the artificial survival of the fittest with genetic operators abstracted from nature to form a robust search mechanism [25].

3.2 Constraint handling

An optimization problem using GAs can be generally expressed as

$$\text{Minimize/Maximize } f(\boldsymbol{x}),\ \boldsymbol{x} = (X_1, X_2, ..., X_n) \in R^n. \quad (1)$$

Under constrain define as

$$\begin{cases} g_i(\boldsymbol{x}) \leqslant 0,\ i = 1,2,...,K \\ h_i(\boldsymbol{x}) = 0,\ j = 1,2,...,P \end{cases}. \quad (2)$$

For structural design optimization, $\boldsymbol{x}$ is an n-dimensional vector called the design vector, representing design variables of n structural components to be optimized, and $f(\boldsymbol{x})$ is the objective function. Also, $g_i(\boldsymbol{x})$ and $h_i(\boldsymbol{x})$ are inequality and quality constrain, respectively. They represent constrains, such as stress and displacement limits to be satisfied by the optimum design.

In GAs, constrains are usually handled using the concept of penalty function as follows:

$$\text{Minimize } \hat{F}_j = F_j(1 + P_j), \quad (3)$$

$$\text{Maximize } \hat{F}_j = F_j(1 - P_j), \quad (4)$$

where $\hat{F}_j$ represents an augmented fitness function after the penalization, P_j is a penalty function whose value is greater than zero for infeasible search space and zero for feasible search space. In this paper the the following form of penalty function is used:

$$P_j = \left(\sum_{j=1}^{K} G_i(x) + \sum_{j=1}^{P} H_i(x)\right)^2, \quad (5)$$

where $G_i(x)$ and $H_i(x)$ represent the degrees of inequality

and equality constraint violations, respectively.

Moreover, in this study for optimization of structures, a fast GA method is utilized. For this purpose, an individual who has more fitness than the other individuals of its current generation is combined with a certain percent of the elitist individuals of the same generation. These new individuals will often have superior features [26]. Figure 3 shows how the proposed GA operates.

4 Modeling and optimization of deployable structures

Modeling and optimization of deployable structures are performed as follows:

Step 1: Modeling of foldable structures can be done: i) By AutoCAD mechanical software, and ii) first drawing it in Formian software to facilitate configuring and then storing it in the mechanical AutoCAD software with *.dwg suffix.

Step 2: Drawing the structure and preparing configurations for analysis in the ABAQUS software by AutoCAD mechanical.

Step 3: Is obtained from the model made in the output AutoCAD with *.IGES suffix for the use of model in the ABAQUS software.

Step 4: Model is analyzed by the ABAQUS software after specifications are allotted to materials and hinges and joints are defined.

In this study, bar elements were modelled as a wire in part module in ABAQUS as well as the beam property was assigned to them. Figures 4 and 5 demonstrate hinges and joints properties in ABAQUS.

Step 5: The structure-forming configuration is first analyzed by the arc length method called RIKS method in Abaqus to verify modeling accuracy.

Step 6: Closing-opening capability of the configuration is controlled in the ABAQUS Software. Figure 6 shows this issue for a 5-sided configuration in the ABAQUS software.

Step 7: All processes and specifications assigned to the model are stored in a text-file with *.jnl suffix containing all model information after structure modeling has been completed in the ABAQUS software.

Step 8: *.jnl suffix is changed to *.py to make *.jnl file generated by MATLAB software readable.

Step 9: For optimization in file *.py, design variables are put in parametric forms so that they can get new values in each iteration.

Step 10: The model file is ready for optimization after doing the above steps and optimization can start hereafter with the optimizer algorithm.

Step 11: MATLAB software writes the values of design variables for each design in each iteration in *.py file, and the model is analyzed with the ABAQUS software with the new values.

Step 12: Such structure responses as stress and displacement are found after the model analysis for each design and the results are read by MATLAB software; the objective function is fined based on the problem

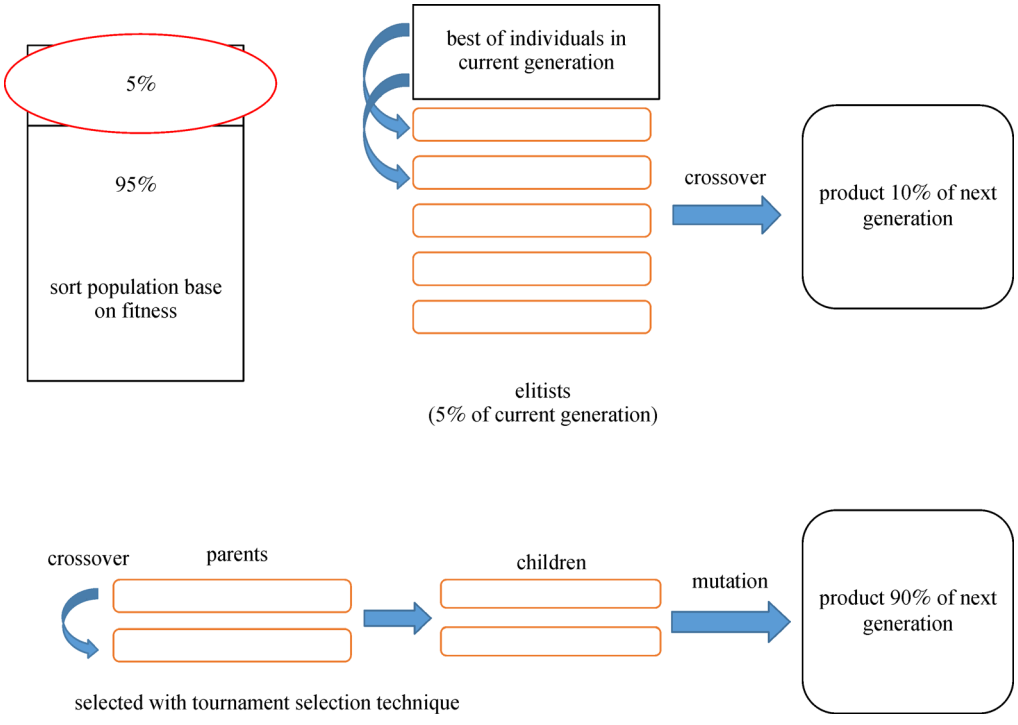

Fig. 3 Selection operator for proposed method [26]

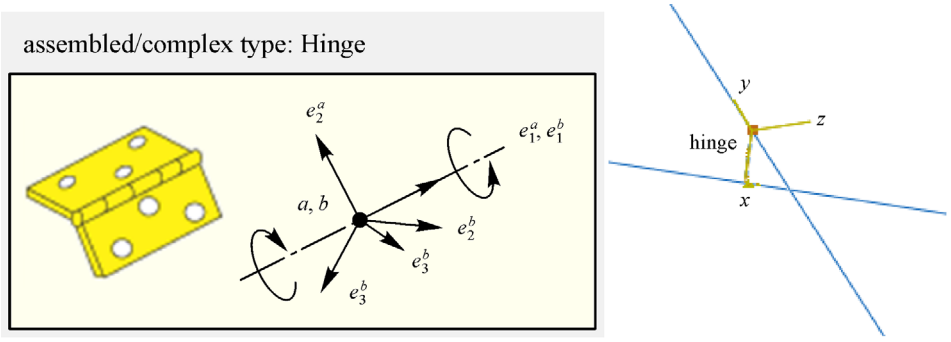

Fig. 4 Hinge properties for scissor elements

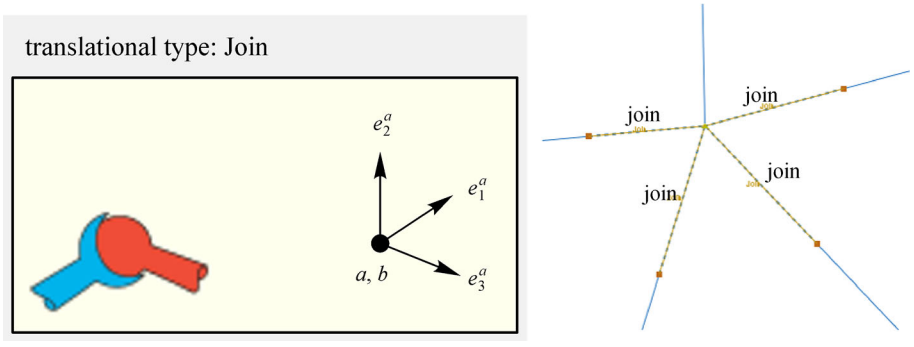

Fig. 5 Join properties for joint connection

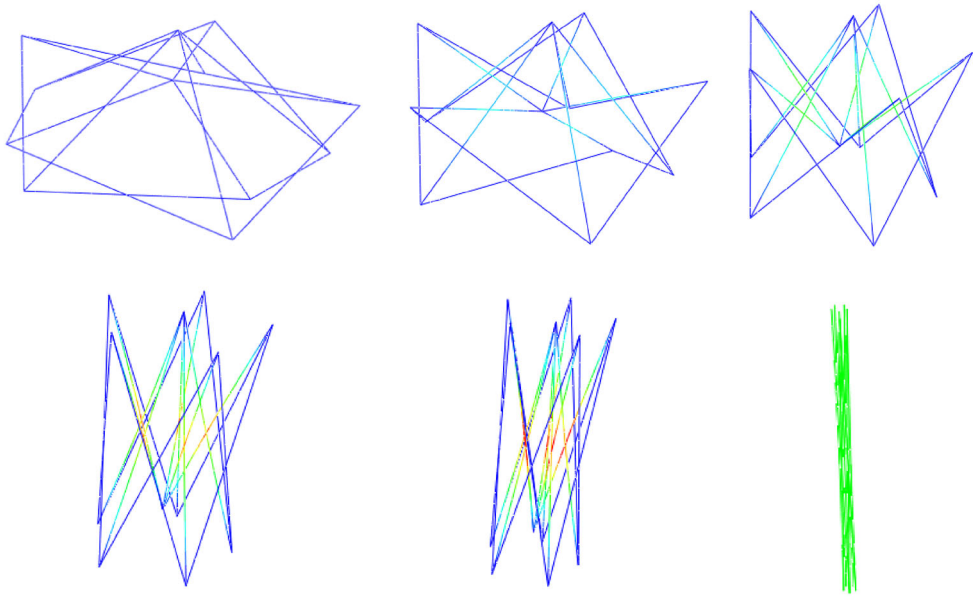

Fig. 6 Successive deformed configurations during deployment of a pentagonal unit

constraints violations.

Step 13: The best design is selected and stored after the fined objective function has been calculated.

Step 14: If the design converges, control of the convergence criterion of the optimization operations will end; otherwise, Steps 11–14 will be repeated.

Figure 7 shows the modeling and optimization flowchart of foldable structures.

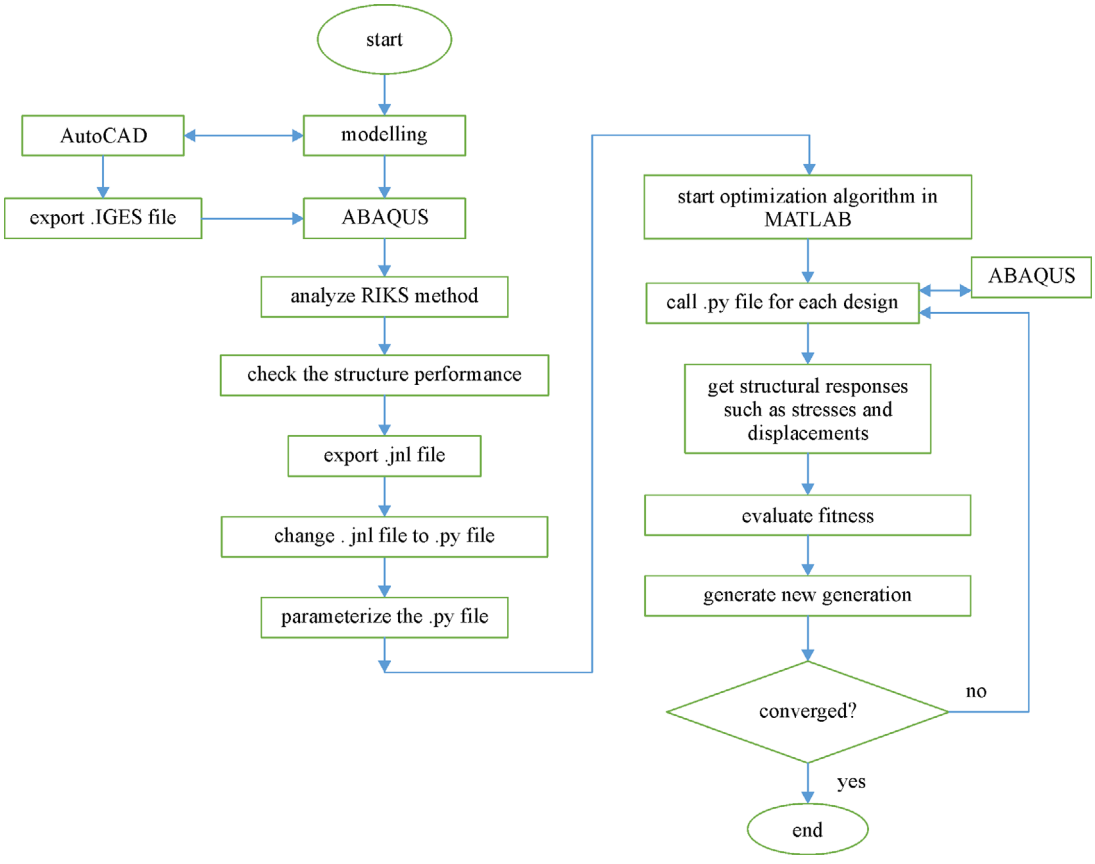

Fig. 7 Flowchart of modelling and optimization of deployable structures

5 Design examples

Size optimization of deployable structures means arriving at optimum values for members' cross-sectional areas A_i that minimize the structure weight W. This minimum design should also satisfy inequality constraints that limit design variable sizes and structural responses [27]. Thus, the optimal design problem may be expressed as

$$\text{Minimize } W(x) = \sum_{i=1}^{n} \rho_i A_i L_i.$$

Subject to

$$\begin{cases} \delta_{\min} \leqslant \delta_i \leqslant \delta_{\max},\ i = 1,\ 2,\ldots,\ m \\ \sigma_{\min} \leqslant \sigma_i \leqslant \sigma_{\max},\ i = 1,\ 2,\ldots,\ n \\ \sigma_i^b \leqslant \sigma_i \leqslant 0,\ i = 1,\ 2,\ldots,\ nc \\ A_{\min} \leqslant A_i \leqslant A_{\max},\ i = 1,\ 2,\ldots,\ ng \end{cases}, \tag{6}$$

where $W(x)$ is the structure weight, n is the number of structure members, m is the number of nodes, nc is the number of compression elements, ng is the number of groups (design variables), ρ_i is the material density of member i, L_i is the length of member i, A_i is the cross-sectional area of member i lying between $A_{\min}$ (lower bound) and $A_{\max}$ (upper bound), σ_i and δ_i are stress and nodal deflection, respectively, and σ_i^b is the allowable buckling stress in member i when it is in compression.

The allowable tensile and compressive stresses are according to AISC ASD (1989) [28] Code, as follows:

$$\begin{cases} \sigma_{\mathrm{t}} = 0.6F_{\mathrm{y}} \ \text{ for } \ \sigma_i \geqslant 0 \\ \sigma_{\mathrm{c}} \ \text{ for } \ \sigma_i < 0 \end{cases}, \tag{7}$$

$$\sigma_{\mathrm{c}} = \begin{cases} \dfrac{F_y}{F.S.}\left(1 - \dfrac{\lambda_i^2}{2C_{\mathrm{c}}^2}\right),\ F.S. = \dfrac{5}{3} + \dfrac{3\lambda_i}{8C_{\mathrm{c}}} - \dfrac{\lambda_i^3}{8C_{\mathrm{c}}^3} \\ \qquad\qquad\qquad\qquad \text{for } \lambda_i < C_{\mathrm{c}} \\ \dfrac{12\pi^2 E}{23\lambda_i^2} \qquad\qquad\qquad\qquad \text{for } \lambda_i \geqslant C_{\mathrm{c}} \end{cases}, \tag{8}$$

$$C_{\mathrm{c}} = \sqrt{\frac{2\pi^2 E}{F_{\mathrm{y}}}}, \tag{9}$$

where σ_{t} is tensile stress, σ_{c} is compressive stress, E is the modulus of elasticity, F_{y} is steel yield stress, C_{c} is the slenderness ratio (λ_i) dividing the elastic and inelastic buckling regions, λ_i is the slenderness ratio ($\lambda_i = kL_i/r_i$), k

is the effective length factor, and r_i is the radius of gyration ($r_i = \sqrt{I/A}$), I is the second moment of area, and A is the cross-sectional area of member.

Specified external wind pressure or suction on part or all of the surface of a structure is found by Eq. (10) [29]:

$$p = I_w q C_e C_g C_p, \tag{10}$$

where p is the specified external pressure that acts statically in a direction normal to the surface either as a pressure towards the surface or as a suction away from the surface, I_w is the wind load importance factor, q is the reference velocity pressure, C_e is the exposure factor, C_g is the gust effect factor, and C_p is the external pressure coefficient averaged over the considered surface area.

Figure 8 shows cross-section of all members. Tables 1 and 2 give section list and material properties for design of examples, respectively.

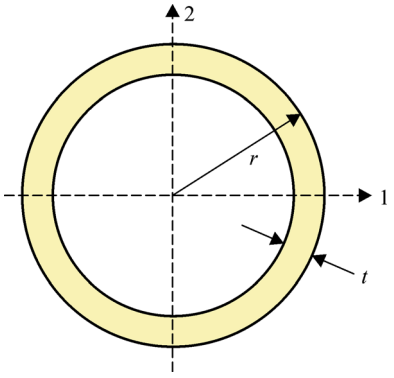

Fig. 8 Elements cross-section

Table 1 Discrete section lists for design of examples

radius (mm)	thickness (mm)
[10 15 20 25 30 35 40 45 50 55 60 65 70 75 80 85 90 95 100]	[1 2 3 4 5 6 7 8 9 10]

Table 2 Material properties for design of examples

material	modulus of elasticity (N/m^2)	density (kg/m^3)	yield stress (MPa)
steel	2×10^{11}	7850	235
aluminum	69×10^9	2700	276

Table 3 contains the proposed GA properties for each example studied. For termination criteria, as commonly considered in metaheuristic algorithms, the best result is calculated where the termination condition may be assumed as the maximum number of iterations, CPU time or ε which is a small non-negative value and is defined as an allowable tolerance between the latest results. In this study, the gas is stopped after 10 iterations while the algorithm could not find any better solution.

Table 3 The proposed GA properties

example	population size	mutation probability	crossover type	selection operator
foldable double layer	40	1	single point	tournament selection
foldable barrel vault	60			
	120			
scissor-like dome	20			

5.1 Foldable double layer

The foldable double layer shown in Fig. 9 is considered as the first example (its Formex function is given in the appendix). In this example, variations include the use of discrete radius/thickness, allowable stress limits in members, and value/location of node deflection constraints. The maximum deflection of any node (in both vertical and horizontal directions) is ± 1 cm and length L for all members is 1.1314 m. All members are linked into two groups (Fig. 9) and the structure is considered to be subjected to wind load according to Eq. (10). In this state, the structure members are grouped into two: 14 intermediate members in one group and 48 in another.

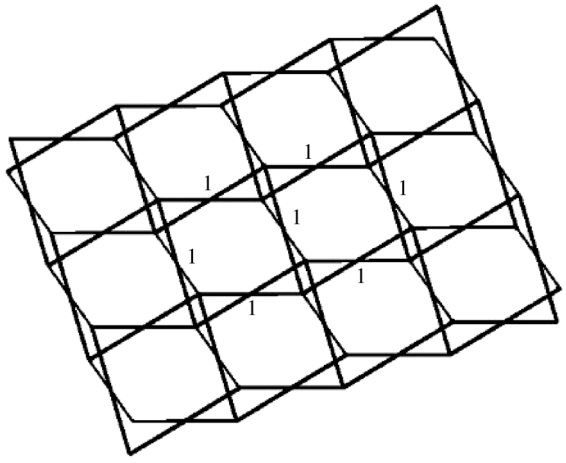

Fig. 9 Group numbers of the foldable double layer

Convergence charts of foldable double layer with two types of cross-sections for steel and aluminum are shown in Figs. 10 and 11, respectively. A comparison of results in Table 4 shows that the aluminum model weight is 59% less than that of the steel model whereas the material consumed in aluminum model is only 5% more than the steel used in the second case.

5.2 Foldable barrel vault

The foldable barrel vault (its Formex function is given in the appendix) has been considered under two cases: 1) All members are linked into two groups (Fig. 12), and 2) all

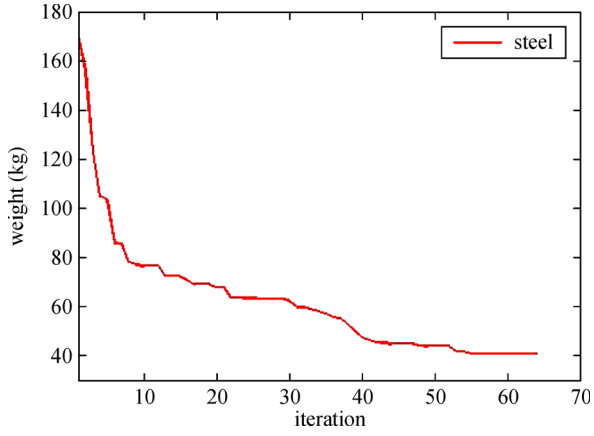

Fig. 10 The convergence history of the foldable double layer with steel material

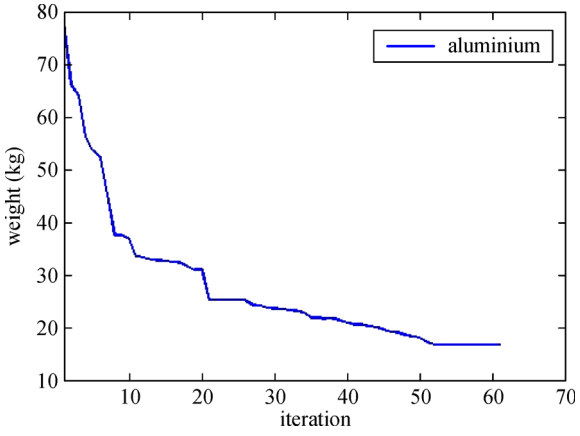

Fig. 11 The convergence history of the foldable double layer with aluminium material

members are linked into six groups (Fig. 13). The structure is considered to be subjected to wind load according to Eq. (10).

Similar to the foldable double layer, the objective, in this problem, is to minimize the structure weight considering section radius and thickness (Table 1) as design variables. Steel and aluminum material specifications are given in Table 2 and Eqs. (6)–(10) have been used to optimize the selected model.

Case 1: Structure members are classified into two groups (Fig. 12). Forty members are in one group and 36 in another.

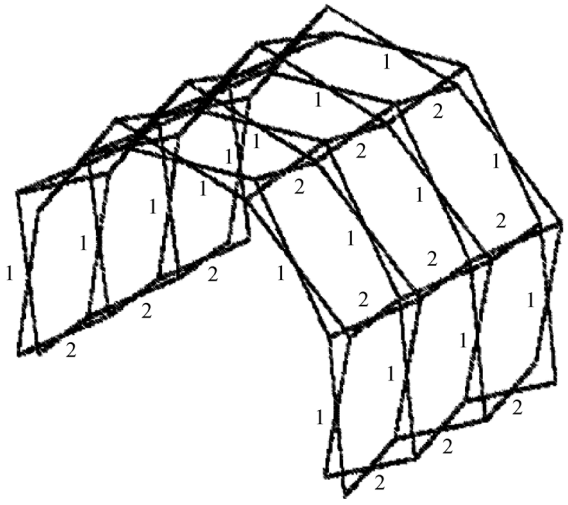

Fig. 12 Group numbers of the foldable barrel vault (Case 1)

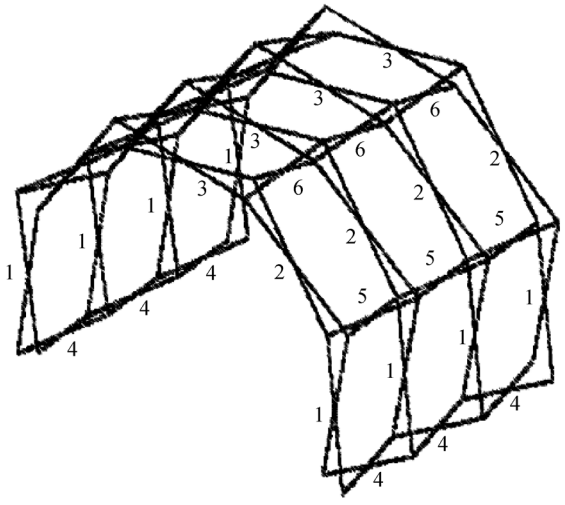

Fig. 13 Group numbers of the foldable barrel vault (Case 2)

Case 2: Structure members are classified into 6 groups (Fig. 13). Members with geometric symmetry are all in one group.

The foldable barrel's convergence history for steel and aluminum (Case 1) is shown in Figs. 14 and 15, respectively. A comparison of the results in Table 5 shows that the aluminum model weight is 42.62% less than

Table 4 Optimization results for a foldable double layer

material	variables	area (cm^2)	radius (mm)	thickness (mm)	weight (kg)	NFE
steel	A_1	1.2252	20	1	40.6812	2560
	A_2	0.5969	10	1		
aluminum	A_1	1.8535	30	1	16.6794	2440
	A_2	0.5969	10	1		

Note: NFE represents the number of function evaluations

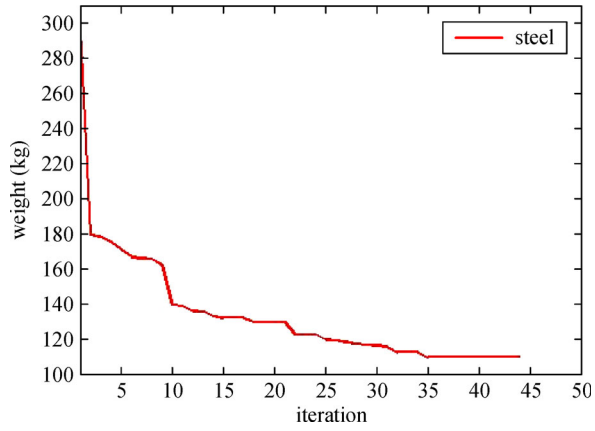

Fig. 14 The convergence history of the foldable barrel vault with steel material (Case 1)

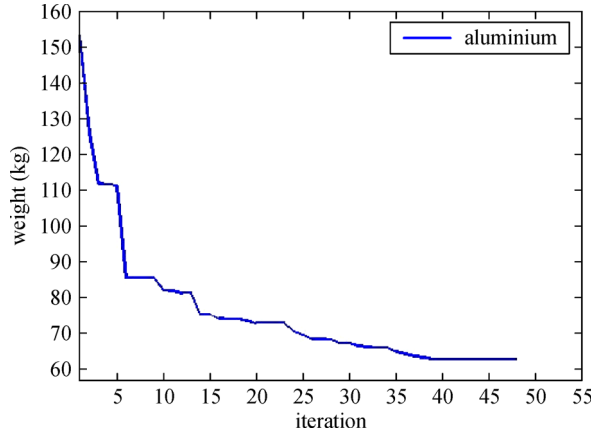

Fig. 15 The convergence history of the foldable barrel vault with aluminium material (Case 1)

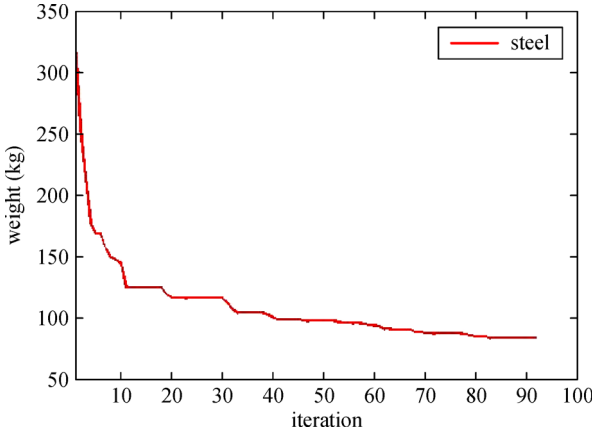

Fig. 16 The convergence history of the foldable barrel vault with steel material (Case 2)

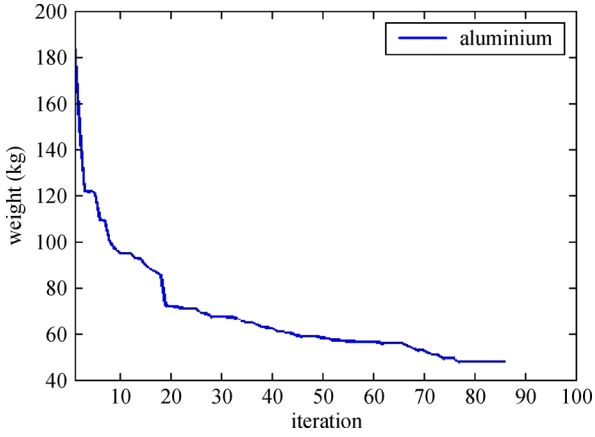

Fig. 17 The convergence history of the foldable barrel vault with aluminium material (Case 2)

that of the steel model whereas the material consumed in the former is 58.88% more than that in the latter.

Convergence charts of foldable barrel for steel and aluminum (Case 2) are shown in Figs. 16 and 17, respectively. A comparison of results in Table 6 shows that the aluminum model weight is 42.61% less than that of the steel model (not differing from that in Case 1) whereas the material consumed in aluminum model is 55.55% more than the steel model which is only 3% less than that in Case 1, hence, when member grouping is increased from 2 to 6, the weight-to-amount ratio of the used material is the same, but the total structure weight is decreased by 25%.

5.3 Scissor-like dome

The geometric design of the scissor-like dome including pentagonal and hexagonal units (Fig. 18) was considered as a last example. Figure 19 shows the characteristic units of this dome.

The scissor-hinge dome convergence history for steel and aluminum is shown in Figs. 20 and 21, respectively. A comparison of the results in Table 7 shows that the aluminum model weight is 65.6% less than that of the steel model which is exactly equal to the density ratio of the two materials considering that member sectional area in both models is equal and minimum, but since aluminum is much more expensive than steel, the latter is suggested for the construction of this structure.

6 Conclusions

In this paper, we have used a fast GA-based method for optimization of three examples of deployable structures including foldable double layer, foldable barrel vault and scissor-like dome. All examples were modeled in ABAQUS software and closing-opening capability of the configuration were checked.

Optimization results of deployable structures showed that despite lower weight of aluminum models compared

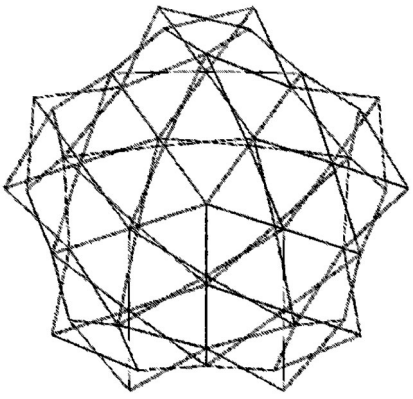

Fig. 18 The deployable dome with scissor-hinge elements

Table 5 Optimization results for a foldable barrel vault (Case 1)

material	variables	area (cm^2)	radius (mm)	thickness (mm)	weight (kg)	NFE
steel	A_1	0.5969	10	1	109.3785	2640
	A_2	1.5394	25	1		
aluminum	A_1	1.2252	20	1	62.7567	2880
	A_2	2.1677	35	1		

Table 6 Optimization results for a foldable barrel vault (Case 2)

material	variables	area (cm^2)	radius (mm)	thickness (mm)	weight (kg)	NFE
steel	A_1	0.5969	10	1	82.7441	11040
	A_2	0.5969	10	1		
	A_3	0.5969	10	1		
	A_4	1.5394	25	1		
	A_5	0.5969	10	1		
	A_6	0.5969	10	1		
aluminum	A_1	1.2252	20	1	47.4886	10320
	A_2	1.2252	20	1		
	A_3	1.2252	20	1		
	A_4	2.1677	35	1		
	A_5	0.5969	10	1		
	A_6	0.5969	10	1		

Table 7 Optimization results for a scissor-like dome

material	area (cm^2)	radius (mm)	thickness (mm)	weight (kg)	NFE
steel	0.5969	10	1	58.0638	260
aluminum	0.5969	10	1	19.9710	240

to steel models, deployable structures made with aluminum are not affordable because they need more material than steel which is environmentally damaging.

Optimization of foldable structures with steel and aluminum showed that when member types in a structure are increased, materials consumed in both models are nearly equal, but steel models are more affordable because aluminum is costlier. It was also concluded that when member types increased, not only the structure weight, but also the consumed materials reduced.

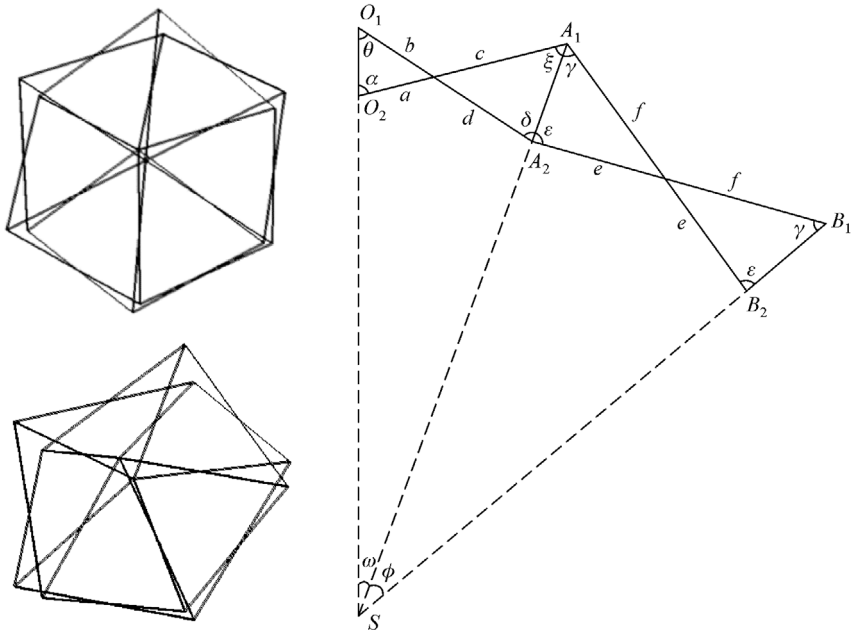

$\theta = 57.0128$ $A_1A_2 = 28$ cm
$\alpha = 91.1629$ $A_2B_2 = 92$ cm
$a = 50.9018$ cm $O_1O_2 = 32$ cm
$b = 60.6721$ cm $\omega = 23.7970$
$c = 52.4174$ cm $\gamma = 62.6736$
$d = 49.0094$ cm $\varepsilon = 85.9521$
$e = 47.7797$ cm $\xi = 67.3659$
$f = 53.6472$ cm $\delta = 80.8098$

$\theta = 53.1001$ $A_1A_2 = 28$ cm
$\alpha = 94.8526$ $A_2B_2 = 92$ cm
$a = 37.6770$ cm $O_1O_2 = 25$ cm
$b = 46.9459$ cm $\omega = 20.0741$
$c = 50.5095$ cm $\gamma = 62.6736$
$d = 50.9173$ cm $\varepsilon = 85.9521$
$e = 47.7797$ cm $\xi = 74.7785$
$f = 53.6472$ cm $\delta = 73.1743$

Fig. 19 Characteristic units for geometric design of deployable scissor-like dome

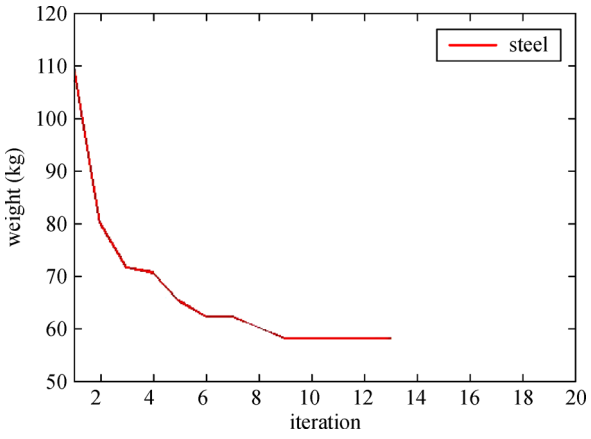

Fig. 20 The convergence history of the foldable dome with steel material

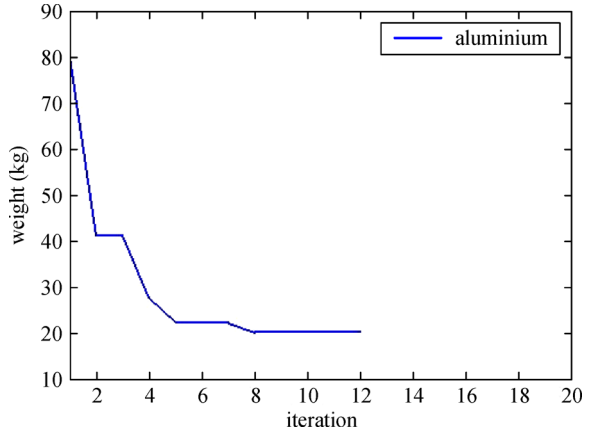

Fig. 21 The convergence history of the foldable dome with aluminium material

Appendix

Formex functions for models are generated by the program Formian based on Formex algebra developed by Nooshin [30].

(*)Foldable Barrel vault(*)

t = 150; (*)control angle(*)

L1 = 0.8; (*) length of upper part of uniplet(*)

L2 = 0.7; (*)length of lower part of uniplet(*)

m = 5; (*)circumferential frequency(*)

n = 3; (*)longitudinal frequency(*)

L = L1 + L2; t1 = 180-t;

D = sqrt|(L1^2 + L2^2-2*L1*L2*cos|t1);

D1 = sqrt|(L^2-D^2);

A = asin|(L2*sin|t1/D);

B = 180 + A-t;

R = D*(sin|B/(sin|B-sin|A));

C = asin|(L*sin|(B/R));

E = rinit(m,n + 1,c,D1)|{[R-D,0,0;R,C,0],[R,0,0;R-D,C,0]}#rinit(m + 1,n,c, D1)|{[R-D,0,0;R,0,D1],[R,0,0;R-D,0,D1]};

F = bc(1,1,1)|E;

P = m*C/2;

BV = verad(0,0,90-P)|F;

Use &,vm(2),vt(2),vh(5,8*R,-12*R,0,0,R,0,1,R);Clear;draw BV;

Radius = R; Depth = D; side = n*D1;

sweep = P; span = 2*R*sin|P; Rise = R*(1-cos|P);

Give Radius, Depth,Side,Sweep,Span,Rise;

(*)Foldable double layer(*)

T = 120; (*) Control angle (*)

D = 0.8; (*) Dimensions of a duplet for T = 90 (*)

m = 4; (*) Frequency in the x-direction (*)

n = 3; (*) Frequency in the y-direction (*)

H = sqrt|2*D*sin|(T/2);

V = sqrt|2*D*cos|(T/2);

Fold = rinid(m,n + 1,H,H)|{[0,0,0; H,0,V],

[0,0,V; H,0,0]}#rinid(m + 1,n,H,H)|

{[0,0,0; 0,H,V], [0,0,V; 0,H,0]};

use &,vn(150,250),vs(35),

vh(m*H, n*H,15*H, 0,0,0, 0,0,1);

clear; draw Fold;

References

1. Gantes C J. Deployable Structures: Analysis and Design. Southampton: Wit Press, 2001
2. Rhode-Barbarigos L G. An active deployable tensegrity structure. Dissertation for the Doctoral Degree. Lausanne: Federal Institute of Technology in Lausanne, 2012
3. Pinero E P. Project for a mobile theatre. Architectural Design, 1961, 12(1): 154–155
4. Chilton J. Space Grid Structures. Abingdon: Taylor & Francis, 2007
5. Friedman N, Farkas G. Roof structures in motion-on retractable and deployable roof structures enabling quick construction or adaption to external excitations. Concrete Structures, 2011, 12: 41–50
6. Gantes C J, Connor J J, Logcher R D, Rosenfeld Y. Structural analysis and design of deployable structures. Computers & Structures, 1989, 32(3–4): 661–669
7. Valcarcef J P, Escrig F. Recent advances in the analysis of expandable structures. In: Escrig F, Brebbia C A, eds. Mobile and Rapidly Assembled Structures II (Vol. 21). Southampton: Computational Mechanics Publications, 1996, 45–54
8. Calatrava S. Study on the foldability of trusses. Dissertation for the Doctoral Degree. Zurich: Swiss Federal Institute of Technology Zurich, 1981
9. Zeigler T R. US Patent 4026313. 1977-05-31
10. Hernández CH, Zalewski W. Expandable structure for the

Venezuelan Pavilion at Expo'92. In: Proceedings of International Conference on Space Structures. 1993, 1710–1719
11. Escrig F. Expandable space frame structures. In: Proceedings of the 3rd International Conference on Space Structures. Guildford: Elsevier, 1984, 845–850
12. Rosenfeld Y, Logcher R D. New concepts for deployable-collapsible structures. International Journal of Space Structures, 1988, 3(1): 20–32
13. Shan W. Foldable space structures. Dissertation for the Doctoral Degree. Surrey: University of Surrey, 1990
14. Langbecker T, Albermani F. Kinematic and non-linear analysis of foldable barrel vaults. Engineering Structures, 2001, 23(2): 158–171
15. Gantes C, Connor J J, Logcher R D. Combining numerical analysis and engineering judgment to design deployable structures. Computers & Structures, 1991, 40(2): 431–440
16. Raphael B, Smith I F. A direct stochastic algorithm for global search. Applied Mathematics and Computation, 2003, 146(2–3): 729–758
17. Dizangian B, Ghasemi M R. A fast marginal feasibility search method in size optimization of truss structures. Asian Journal of Civil Engineering, 2015, 16(5): 567–585
18. Dizangian B, Ghasemi M R. Ranked-based sensitivity analysis for size optimization of structures. Journal of Mechanical Design, 2015, 137(12): 121402
19. Imai K, Schmit L A. Configuration optimization of trusses. Journal of the Structural Division, 1981, 107(5): 745–756
20. Ghasemi H, Park H S, Rabczuk T. A multi-material level set-based topology optimization of flexoelectric composites. Computer Methods in Applied Mechanics and Engineering, 2018, 332: 47–62
21. Nanthakumar S S, Lahmer T, Zhuang X, Park H S, Rabczuk T. Topology optimization of piezoelectric nanostructures. Journal of the Mechanics and Physics of Solids, 2016, 94: 316–335
22. Ghasemi H, Park H S, Rabczuk T. A level-set based IGA formulation for topology optimization of flexoelectric materials. Computer Methods in Applied Mechanics and Engineering, 2017, 313: 239–258
23. Nanthakumar S S, Zhuang X, Park H S, Rabczuk T. Topology optimization of flexoelectric structures. Journal of the Mechanics and Physics of Solids, 2017, 105: 217–234
24. Holland J H. Adaptation in Natural and Artificial Systems: An Introductory Analysis with Applications to Biology, Control, and Artificial Intelligence. Cambridge: MIT Press, 1992
25. Ghasemi M R, Hinton E, Wood R D. Optimization of trusses using genetic algorithms for discrete and continuous variables. Engineering Computations, 1999, 16(3): 272–303
26. Salar M, Ghasemi M R, Dizangian B. A fast GA-based method for solving truss optimization problems. International Journal of Optimization in Civil Engineering, 2015, 6(1): 101–114
27. Lee K S, Geem Z W. A new structural optimization method based on the harmony search algorithm. Computers & Structures, 2004, 82 (9–10): 781–798
28. American Institute of Steel Construction (AISC). Manual of Steel Constructional Low Able Stress Design. 9th ed. Chicago: American Institute of Steel Construction, 1989
29. National Building Code of Canada. Canadian Commission on Building and Fire Codes. Volume 1. 2005
30. Nooshin H, Disney P. Formex configuration processing II. International Journal of Space Structures, 2001, 16(1): 1–56